# Orienting coupled quantum rotors by ultrashort laser pulses

Hiroyuki Shima and Tsuneyoshi Nakayama

*Department of Applied Physics, Graduate School of Engineering, Hokkaido University, Sapporo 060-8628, Japan*

We pointed out that the nonadiabatic orientation of quantum rotors, produced by ultrashort laser pulses, is remarkably enhanced by introducing dipolar interaction between the rotors. This enhanced orientation of quantum rotors is in contrast with the behavior of classical paired rotors, in which dipolar interactions prevent the orientation of the rotors. We demonstrate also that a specially designed sequence of pulses can most efficiently enhance the orientation of quantum paired rotors.

## I. INTRODUCTION

Considerable attention has been paid to the ability of intense laser fields to align or orient polar molecules; in such fields, the molecules experience torque arising from the dipolar interaction with electric fields [1]. One approach to achieve adiabatic molecular alignment is to use a nanosecond-pulse laser [2–4]. While adiabatic alignment disappears after the pulse is turned off, ultrashort pulses (100 fs or less) can excite rotational wave packets of quantum rotors, thus yielding a noticeably aligned shape after the pulse is off [5–11]. Furthermore, a specially designed sequence of pulses is known to achieve an enhanced angular focusing in quantum rotors [12,13]; this has been realized experimentally in optical lattices [14]. These types of alignment, which differ from the adiabatic, are important for manifold applications requiring transient molecular alignment under field-free conditions, such as the generation of laser pulses [15,16] and the control of high harmonic generation as a source of coherent radiation [17].

In most studies of the molecular alignment, dipolar interaction between polar molecules has been neglected. In this case, the rotational dynamics of polar molecules can be simply analyzed by using an isolated kicked-rotor model [18]. The quantum kicked rotor and its classical analog have long served as a paradigm for quantum and classical chaos. In contrast, the quantum dynamics of *interacting* kicked rotors has been less well studied so far, though intriguing phenomena of interacting quantum rotors are expected to emerge. Very recently, a study of the center-of-mass motion in two coupled kicked rotors has revealed that the decoherence effect induced by the internal degree of freedom enhances the quantum-classical correspondence in the dynamics of rotors [19]. In addition, anomalous dielectric responses have been pointed out in two coupled dipolar rotors [20]. These results imply that coupled kicked rotors, even in *only two* rotors, exhibit peculiar behaviors different from those of isolated kicked rotors.

In the present work, we theoretically investigate the quantum dynamics of coupled (paired) kicked rotors subject to an ultrashort laser pulse ($\delta$-function kick). We find that the dipolar interaction between rotors remarkably enhances the transient orientation of paired rotors produced by a $\delta$ kick. This enhancement of the orientation of *quantum* rotors contrasts with the results with the *classical* treatment for paired

rotors; in the latter case, the dipolar interaction inevitably hinders the orientation of coupled rotors. Furthermore, we demonstrate that the orientation of paired rotors can be further enhanced by applying the accumulative squeezing scheme proposed in Ref. [12]. Our findings enlighten the study of transient orientation of interacting polar molecules.

This paper is organized as follows. Section II describes the Hamiltonian of the paired-rotor system together with its analytical solutions for eigenenergies and their eigenfunctions. The time development of paired rotors for *post*-kicked times is given in this section. Section III analyzes the time dependence of the orientation factor in both quantum and classical paired rotors. The physical origin of the enhanced orientation in quantum rotors is discussed on the basis of the spatial profile of the probability density of paired-rotor wave functions. Section IV gives the conclusion. The paper contains two Appendices with the details of the calculations.

## II. PAIRED-ROTOR SYSTEMS

### A. The Hamiltonian

Suppose that two rotors carrying dipole moments $\boldsymbol{\mu}$ are arranged as shown in Fig. 1. For arrangement (a), both rotors
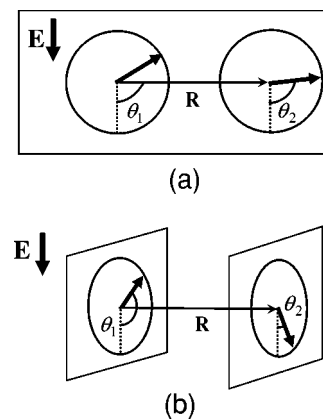


FIG. 1. Definitions of arrangements of two dipolar rotors: (a) two dipoles rotate in an identical plane and (b) two rotors belong to an identical rotation axis. In both cases, the rotors are separated by $R$ and interact via the dipolar interaction $W_{12}$. The direction of the electric field $\boldsymbol{E}(t)$ is defined as shown.

rotate in a plane, while in the case of (b), both rotors belong to an identical rotation axis [21]. The Hamiltonian for the system is given by $H=H_1+H_2+W_{12}$, where $H_i$ is the Hamiltonian for the $i$th kicked rotor and $W_{12}$ represents dipolar interaction between rotors. The term $H_i$ can be written as

$$H_i = \frac{L_i^2}{2I} + V(\theta_i, t), \quad (1)$$

where $L_i$ is the angular momentum operator and $I$ is the moment of inertia of the rotor. When rotors are driven by a linearly polarized field, we can set

$$V(\theta_i, t) = -\mu E(t)\cos(\theta_i), \quad (2)$$

where $E(t)$ is the field amplitude of short laser pulses. The direction of the field is fixed as shown in Fig. 1, causing the angular focusing of paired rotors at $\theta_1=\theta_2=0$. Assuming that the rotational radius of rotors is sufficiently smaller than the separation $R$ between rotors, the dipolar interaction $W_{12}$ is expressed by

$$W_{12} = \frac{1}{4\pi\varepsilon R^3}\left[\boldsymbol{\mu}_1 \cdot \boldsymbol{\mu}_2 - 3\frac{(\boldsymbol{\mu}_1 \cdot \boldsymbol{R})(\boldsymbol{\mu}_2 \cdot \boldsymbol{R})}{R^2}\right] \quad (3)$$

with the dielectric constant $\varepsilon$. The vector $\boldsymbol{R}$ connects two rotational centers as denoted in Fig.1. For simplicity, we re-write the term (3) as

$$W_{12} = E_D \cdot F(\theta_1, \theta_2) \quad (4)$$

with the definition

$$E_D = \frac{\mu^2}{4\pi\varepsilon R^3}. \quad (5)$$

The quantity $E_D$ determines the magnitude of the dipolar interaction between rotors, and plays a key role in the dynamics of coupled rotors, as we discuss later. The explicit form of $F(\theta_1, \theta_2)$ is obtained straightforwardly from Fig.1. The arrangement (a) gives the form

$$F(\theta_1, \theta_2) = \cos\theta_1\cos\theta_2 - 2\sin\theta_1\sin\theta_2, \quad (6)$$

while, for arrangement (b), we have

$$F(\theta_1, \theta_2) = \cos\theta_1\cos\theta_2 + \sin\theta_1\sin\theta_2$$
$$= \cos(\theta_1 - \theta_2). \quad (7)$$

### B. Eigenenergies and their eigenfunctions

In the absence of the field $E(t)$, eigenstates of paired rotors are analytically obtained by transforming variables into $\xi=(\theta_1+\theta_2)/2$ and $\eta=(\theta_1-\theta_2)/2$. Substituting them into Eqs. (1) and (4), the Hamiltonian $H$ is separated as [20]:

$$H = H_\xi + H_\eta, \quad (8)$$

$$H_\alpha = -\frac{E_K}{2}\frac{\partial^2}{\partial\alpha^2} + E_D c_\alpha \cos 2(\alpha+\alpha_0); \quad \alpha=\xi,\eta. \quad (9)$$

Here the quantity $E_K \equiv \hbar^2/(2I)$ represents the kinetic energy. The parameters $(c_\xi, c_\eta, \xi_0, \eta_0)$ equal $(3/2, 1/2, 0, \pi/2)$ for

arrangement (a) and $(0, 1, 0, 0)$ for (b). The separability of the Hamiltonian $H$ allows us to write the paired-rotor wave function in the form $\Psi(\xi, \eta) = \varphi_\xi(\xi)\varphi_\eta(\eta)$. Consequently, the Schrödinger equation of paired rotors $H\Psi(\xi, \eta) = E\Psi(\xi, \eta)$ can be decomposed into two independent eigenvalue equations expressed by

$$\frac{\partial^2\varphi_\alpha}{\partial\alpha^2} + [\varepsilon_\alpha - 2v_\alpha\cos 2(\alpha+\alpha_0)]\varphi_\alpha = 0; \quad \alpha=\xi,\eta, \quad (10)$$

where $\varepsilon_\alpha = 2E_\alpha/E_K$ and $v_\alpha = c_\alpha E_D/E_K$. The solution of Eq. (10) is given by the Mathieu function [22], whose explicit forms are given in Appendix A. The eigenenergies $E$ of paired rotors are thus expressed by $E=(\varepsilon_x+\varepsilon_y)E_K/2$.

### C. Time development of wave functions

Let us consider the time development of the wave function in paired-rotor systems after a $\delta$-function kick at $t=\tau$. The wave function $\Psi(\theta_1, \theta_2, \tau^+)$ immediately after the kick is related to that just before the kick, $\Psi(\theta_1, \theta_2, \tau^-)$, with a phase determined by

$$\Psi(\theta_1, \theta_2, \tau^+) = \exp\left\{\int_{-\infty}^\infty -\frac{i}{\hbar}[V(\theta_1, t) + V(\theta_2, t)]dt\right\}\Psi(\theta_1, \theta_2, \tau^-). \quad (11)$$

Substituting definition (2) into Eq. (11) and transforming variables $(\theta_1, \theta_2) \to (\xi, \eta)$, we obtain

$$\Psi(\xi, \eta, \tau^+) = \sum_{n=-\infty}^\infty i^n J_n\left(\frac{2P}{\hbar}\cos\xi\right)\exp(-in\eta)\Psi(\xi, \eta, \tau^-), \quad (12)$$

where $J_n(z)$ is the Bessel function of $n$th order. The quantity

$$P = \int_{-\infty}^\infty \mu E(t)dt \quad (13)$$

represents the strength of the pulse. In actual calculations for Eq. (12), the summation of $n$ can be truncated at the finite value $\pm n_c$, since the magnitude of the Bessel function $J_n[(2P/\hbar)\cos\xi]$ rapidly decays with increasing $|n|$. The time development of paired rotors for *post*-kicked times is described by

$$\Psi(\xi, \eta, \tau^+ + t) = \exp\left[-\frac{i}{\hbar}(H_\xi + H_\eta)t\right]\Psi(\xi, \eta, \tau^+). \quad (14)$$

The right-hand side of Eq. (14) can be analytically calculated by expanding the function $\Psi(\xi, \eta, \tau^+)$ by the Mathieu function. The details of the calculation are presented in Appendix B. In the following, we set $\tau=0$, and take $E_K$ and $\hbar/E_K$ as units of energy and time, respectively. The initial state just before the kick is fixed in the ground state.
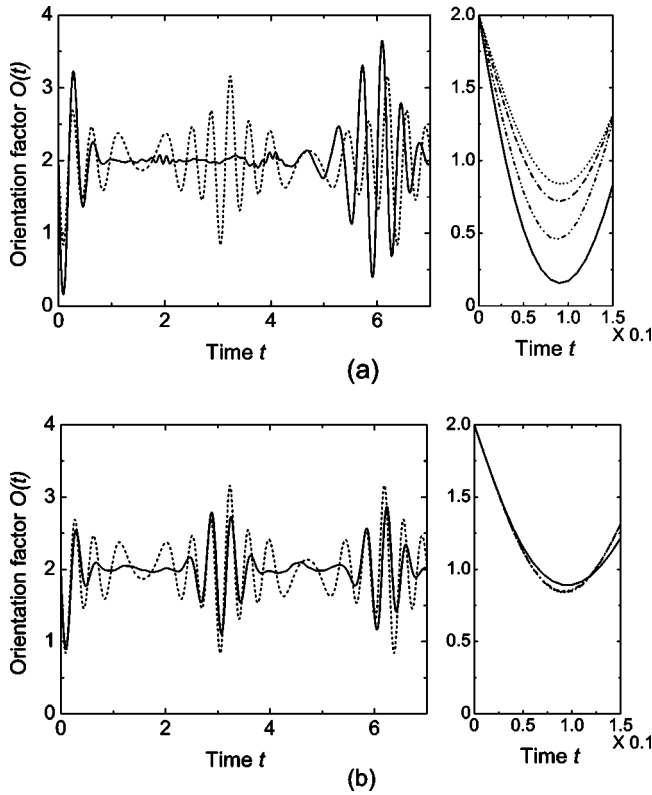
FIG. 2. The orientation factor $O(t)$ in quantum paired rotors. The figures (a) and (b) correspond to arrangements (a) and (b) in Fig. 1. The quantity $\hbar/E_K$ is taken as the unit of time. Left: The time dependence for $O(t)$ within a long time scale. The parameter $\Gamma$ is varied as $\Gamma=0$ (dotted line) and $\Gamma=30.0$ (solid line) fixing the kick strength $P=10$. Right: The behavior of $O(t)$ within a short time scale. $\Gamma$ is varied as $\Gamma=0$ (dotted line), $\Gamma=1.0$ (dashed-dotted), $\Gamma=3.0$ (dashed-dotted-dotted), and $\Gamma=30.0$ (solid).

### III. ORIENTATION OF PAIRED ROTORS

#### A. The orientation factor

The degree of orientation for paired rotors is characterized by the orientation factor $O(t)=\langle 2-\cos\theta_1-\cos\theta_2\rangle$, where the angular brackets indicate to take the expectation value. The factor $O(t)$ tends to be zero when the orientation of the rotors in the field direction of $E$ is perfect. On the other hand, the factor equals 2 when the amplitude of wave function $|\Psi(\theta_1,\theta_2)|$ is uniformly distributed in the $\theta_1$-$\theta_2$ space. The strength of the dipolar interaction is characterized by the parameter $\Gamma=E_D/E_K$, i.e., the ratio of the interaction energy $E_D$ to the kinetic energy $E_K$.

Figures 2(a) and 2(b) show the time dependence for the orientation factor $O(t)$ for paired rotors fixing the kick strength $P=10$. Indices (a) and (b) in Fig. 2 correspond to arrangement of rotors (a) and (b) in Fig. 1. In both (a) and (b), the left figure plots the orientation factor for a long time scale, $0\leq t\leq 7.0$, while the right one does so for a short time scale, $0\leq t\leq 0.15$. We first discuss the two figures on the left, where two values of $\Gamma$ are taken; the dotted lines display the orientation factor for $\Gamma=0$, and the solid lines display that for $\Gamma=30.0$. For $\Gamma=0$, the time dependence for $O(t)$ for arrangement (a) is identical to that for (b), because the two

rotors are no longer correlated via dipolar interaction. In this case, the orientation factor yields a simple form [23] of

$$O(t)=2-2J_1(2P\sin t) \qquad (15)$$

with the lowest value of $O(t_c)=0.836$ at the focal time $t=t_c=9.2\times 10^{-2}$.

For finite $\Gamma$'s, the orientation factor exhibits somewhat complicated behavior different from that for isolated rotors. The left two figures in Fig. 2 exhibit the difference of the time dependence for $O(t)$ between the case of $\Gamma=30.0$ and that of $\Gamma=0$. For arrangement (a), the magnitude of $O(t)$ for $\Gamma=30.0$ exceeds that for $\Gamma=0$ at a time $t\approx 0$ and $t\approx 2\pi$. We must notice that the lowest value of $O(t)$ for $\Gamma=30.0$ located at $t=t_c\approx 0.1$ is remarkably smaller than that for $\Gamma=0$. This indicates that, in arrangement (a), the orientation of paired rotors is enhanced by introducing strong dipolar interaction. For arrangement (b), in contrast, the magnitude of $O(t)$ for $\Gamma=30.0$ does not exceed that for $\Gamma=0$ at any $t$. In addition, the lowest value of $O(t)$ at $t\approx 0.1$ seems to be invariant to the change of $\Gamma$, implying that the orientation of paired rotors in arrangement (b) is not much affected by dipolar interaction.

In order to examine the effect of the interaction for the lowest value of $O(t)$, we investigate in detail the behavior of $O(t)$ around the focal time $t_c$ with varying $\Gamma$. The calculated results are shown in the right two images in Fig. 2, where the value of $\Gamma$ is increased from $\Gamma=0$ (dotted line) up to $\Gamma=30.0$ (solid line). In case (a), the increase in $\Gamma$ monotonously reduces the lowest value of $O(t)$. For $\Gamma=30.0$, the factor eventually takes the lowest value $O(t_c)=0.156$ at the focal time $t_c=9.1\times 10^{-2}$, which is much smaller than the lowest value of $O(t)$ for $\Gamma=0$. In case (b), on the other hand, the time dependence for $O(t)$ hardly changes with varying $\Gamma$. We thus conclude that, as far as arrangement (a) is concerned, the orientation of paired rotors can be efficiently enhanced by taking into account the dipolar interaction between rotors. This is one of main findings of the present study. As we see in the next subsection, the enhanced orientation in *quantum* rotors cannot be interpreted from the *classical* dynamics for paired rotors, indicating that the enhanced orientation stems from a purely quantum effect.

#### B. Classical paired rotors

Before proceeding to a further investigation of *quantum* paired rotors, we consider the effect of dipolar interaction on the orientation for *classical* paired rotors. For classical kicked rotors, the term $H_i$ defined in (2) is rewritten as

$$H_i=\frac{I}{2}\dot{\theta}_i^2(t)+V(\theta_i,t), \qquad (16)$$

while the interaction term $W_{ij}$ is the same as that defined in (4). Under field-free conditions, the equations of motion for arrangement (a) are given by

$$I\ddot{\theta}_1=\frac{E_D}{2}[3\sin(\theta_1+\theta_2)-\sin(\theta_1-\theta_2)], \qquad (17)$$
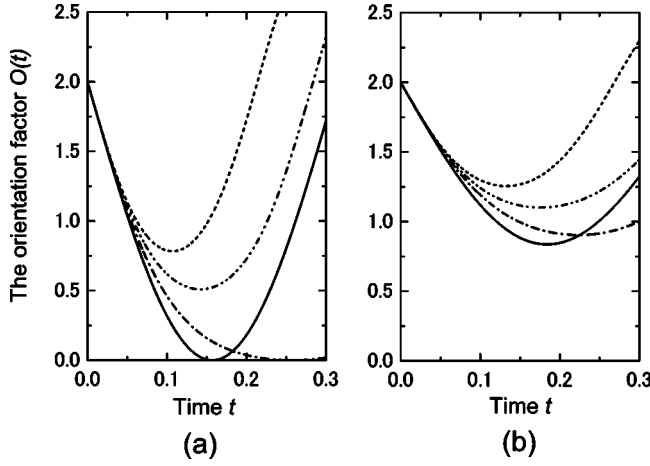
FIG. 3. The orientation factor $O(t)$ in classical paired rotors. Figures (a) and (b) correspond to arrangements (a) and (b) in Fig. 1. The quantity $I/P$ is taken as the unit of time. The parameter $\Gamma_{\mathrm{cl}} = E_D/(2I)$, determining the strength of dipolar interaction, is varied as $\Gamma_{\mathrm{cl}} = 0, 15, 30, 45$ from the bottom (solid line) to the top (dashed line).

$$I\ddot{\theta}_2 = \frac{E_D}{2}[3\sin(\theta_1 + \theta_2) + \sin(\theta_1 - \theta_2)]. \quad (18)$$

By transforming the variables into $q_1 = \theta_1 + \theta_2$ and $q_2 = \theta_1 - \theta_2$, we obtain the following equations:

$$\ddot{q}_1(t) = 6\Gamma_{\mathrm{cl}} \sin q_1(t), \quad (19)$$

$$\ddot{q}_2(t) = -2\Gamma_{\mathrm{cl}} \sin q_2(t). \quad (20)$$

Here we define the parameter $\Gamma_{\mathrm{cl}} = E_D/(2I)$, showing the strength of the dipolar interaction between classical rotors. For arrangement (b), the same procedure yields

$$\ddot{q}_1(t) = 0, \quad (21)$$

$$\ddot{q}_2(t) = 4\Gamma_{\mathrm{cl}} \sin q(t). \quad (22)$$

Solutions of Eqs. (19)–(22) are expressed by Jacobi's elliptic functions. The orientation factor for classical paired rotors is calculated by $O(t) = 2 - 2\langle \cos q_1(t) \cos q_2(t) \rangle_{\mathrm{cl}}$, where the bracket $\langle \cdots \rangle_{\mathrm{cl}}$ means averaging over initial angles $\theta_i(t=0)$ [24].

Figure 3 shows the time dependence of the orientation factor for the classical paired rotors. Quantities $I/P$ and $(I/P)^2$ are taken as the unit of time and the parameter $\Gamma_{\mathrm{cl}}$, respectively. The value of $\Gamma_{\mathrm{cl}}$ is incrementally increased from $\Gamma_{\mathrm{cl}} = 0$ (dotted line) up to $\Gamma_{\mathrm{cl}} = 45$ (solid line) as denoted in the figure caption. We see that the increase in $\Gamma_{\mathrm{cl}}$ inevitably raises the minimal value of $O(t)$ in both arrangements (a) and (b). This leads to the conclusion that, in *classical* systems, the strong dipolar interaction interferes with the orientation of paired rotors for both arrangements (a) and (b). The physical interpretation is given as follows. When two dipolar rotors are assigned in arrangement (a), strong dipolar interaction forces them to be parallel in the direction normal to the field direction (see Fig. 1). Hence, the interaction hinders the
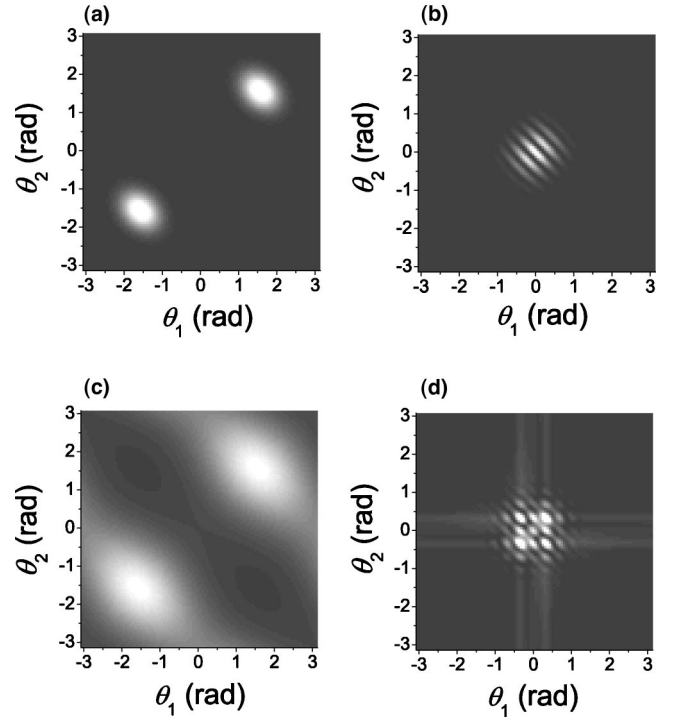


FIG. 4. Contour plots of the probability density $|\Psi(\theta_1, \theta_2, t)|^2$ for arrangement (a) in Fig. 1. Top: The parameter $\Gamma = 30.0$ with (a) $t=0$, and (b) $t=t_c$. Bottom: $\Gamma = 1.0$ with (c) $t=0$, and (d) $t=t_c$. White regions indicate large amplitudes of the probability density.

orientation of rotors in the field direction. For arrangement (b), on the other hand, two dipolar rotors tend to be antiparallel to each other. This increases the minimal orientation factor at the focal time. As a consequence, the dipolar interaction in *classical* systems certainly prevents the rotors from becoming oriented in the field direction defined in Fig. 1.

These facts naturally lead us to the following question: Why is it that a strong dipolar interaction can enhance the orientation of rotors in *quantum* systems [see Fig. 2(a)]? Comparing the behavior of $O(t)$ shown in Fig. 3(a) with that shown in the right of Fig. 2(a), we clearly see that the effect of dipolar interaction on the orientation of paired rotors differs completely between classical and quantum systems. To settle this point, we consider the time development of wave functions in the paired-rotor system as follows.

### C. Time development of wave functions for postkicked time

To understand the mechanism underlying the enhanced orientation in quantum paired rotors, we examine the time development of the probability density $|\Psi(\theta_1, \theta_2, t)|^2$ in the $\theta_1 - \theta_2$ space. Figures 4(a) and 4(b) give contour plots of the probability density for arrangement (a) with $\Gamma = 30.0$. At $t=0$ [Fig. 4(a)], the amplitude of $|\Psi(\theta_1, \theta_2, t)|^2$ is spatially confined around the two symmetric positions $(\theta_1, \theta_2) = (\pi/2, \pi/2)$ and $(-\pi/2, -\pi/2)$. When the kick is applied, these two wave packets move toward the origin $\theta_1 = \theta_2 = 0$ while retaining their shapes, and finally collide head-on with each other at the origin at a focal time $t=t_c$. The resultant angular focusing is demonstrated in Fig. 4(b), where the

probability density of $|\Psi(\theta_1,\theta_2)|^2$ is well localized at around the origin. This transient angular focusing at the origin enhances the orientation of quantum paired rotors.

We must note that angular focusing is enhanced only when $\Gamma \gg 1$, namely, when the two rotors are strongly correlated via dipolar interaction. If the dipolar interaction is sufficiently weak ($\Gamma \leq 1$), the probability density for the initial state is broadly distributed in the $\theta_1$-$\theta_2$ plane [Fig. 4(c)]. After a kick is applied, the amplitude of the wave function spreads out over the $\theta_1$-$\theta_2$ space, followed by the formation of a "rainbow structure" [12] at a focal time $t_c$ [Fig. 4(d)]. The degree of angular focusing for the rainbow structure is obviously inferior to that for the case of strongly interacting rotors [Fig. 4(b)]. In summary, two factors are essential for enhancing the orientation of paired rotors: (i) The initial state before the kick consists of two wave packets strongly confined at symmetric positions with respect to the origin; (ii) these wave packets move translationally toward the origin after the kick. It should be mentioned that the translational motion of two wave packets after a $\delta$ pulse is not trivial. We can analytically trace the motion of those wave packets by calculating the expansion coefficients $D_{ll'}$ appearing in Appendix B. Details of the calculations will be published elsewhere [25].

The spatial profile of the initial eigenstate is determined by the potential term $W_{12}$. For arrangement (a), the potential $W_{12}$ as a function of $\theta_1$ and $\theta_2$ gives two potential minima, at $(\theta_1,\theta_2)=(\pi/2,\pi/2)$ and $(-\pi/2,-\pi/2)$, and a maximum at $(\theta_1,\theta_2)=(0,0)$ [20]. The energy difference between the minimum and the maximum is determined by the interaction energy $E_D$ or, equivalently, the parameter $\Gamma=E_D/E_K$. When $\Gamma$ is much larger than unity, the energy difference becomes so large that the initial eigenstate is strongly localized at the two potential minima, as shown in Fig. 4(a). In addition, the amplitude of the wave function at the origin becomes almost zero due to the large potential maximum. For postkicked time, however, the kick creates a large number of excited states, so that a superposition of them can produce a transient angular focusing at the potential maximum $(\theta_1,\theta_2)=(0,0)$. This leads to a minimal orientation factor at a focal time. On the other hand, in the *classical* limit, the orientation of paired rotors in the field direction $(\theta_1,\theta_2)=(0,0)$ cannot occur when the energy difference between the minimum and the maximum is larger than the kinetic energy of the rotors immediately after the kick. In other words, the strong dipolar interaction prevents the paired-rotor state from being located at the origin $(\theta_1,\theta_2)=(0,0)$. This follows that the enhanced orientation of paired rotors is a purely quantum phenomenon.

### D. The accumulative squeezing

The orientation of paired rotors can be further enhanced by applying the "accumulative squeezing" scheme proposed in Ref. [12] . This strategy is based on a specially designed series of short laser pulses leading to a dramatic narrowing of the rotor angular distribution. Figure 5 shows the orientation factor $O(t)$ of paired rotors kicked by a sequence of seven pulses of the strength $P=10$. The values of $\Gamma$ increase from 0 (solid) to 30.0 (dotted). For both arrangement, the strategy
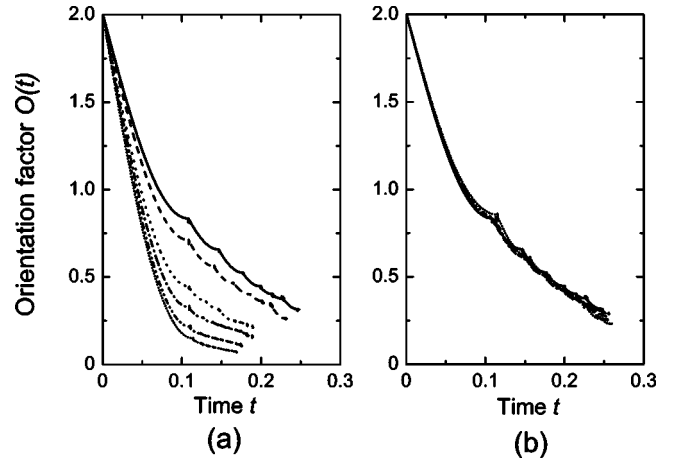


FIG. 5. The orientation factor $O(t)$ for paired rotors kicked with a sequence of seven pulses of the strength $P=10$. The values of $\Gamma$ are varied as $\Gamma=0$, 1.0, 3.0, 5.0, 10.0, 30.0 from the top (the solid line) to the bottom (the dotted one). The quantity $\hbar/E_K$ is taken as unit of time.

works well to achieve the angular squeezing in paired rotors. Moreover, in arrangement (a), a considerable reduction of the factor $O(t)$ is seen for strongly interacting paired rotors with $\Gamma \gg 1$. This result provides a prospect for the scheme of multiple-pulse angular squeezing in interacting quantum rotors.

### IV. CONCLUSION

In conclusion, we have theoretically investigated the quantum dynamics of paired kicked rotors. The orientation of paired rotors after the $\delta$-function kick is remarkably enhanced by introducing dipolar interaction between rotors, when the rotors are deposited in an identical plane. The enhanced orientation is attributable mainly to two factors: (i) The initial state before the kick consists of two wave packets strongly confined at symmetric positions with respect to the origin in the $\theta_1$-$\theta_2$ space; (ii) These wave packets move translationally toward the origin after the kick. We have also demonstrated that the orientation of quantum paired rotors can be further enhanced by applying a specially designed sequence of pulses. Our findings will stimulate experimental works aimed at the orientation of polar molecules correlated via dipolar interaction.

### ACKNOWLEDGMENTS

### APPENDIX A: EXPANSION OF MATHIEU FUNCTIONS

Four kinds of Mathieu functions, $ce_{2n}$, $se_{2n+1}$, $ce_{2n+1}$, and $se_{2n+2}$, can be expressed in terms of the Fourier expansion as follows [22]:

$$\mathrm{ce}_{2n}(\alpha, v_\alpha) = \sum_{m=0}^{\infty} A_{2m}^{(2n)}(v_\alpha)\cos 2m\alpha, \tag{A1}$$

$$\mathrm{se}_{2n+1}(\alpha, v_\alpha) = \sum_{m=0}^{\infty} B_{2m+1}^{(2n+1)}(v_\alpha)\sin(2m+1)\alpha, \tag{A2}$$

$$\mathrm{ce}_{2n+1}(\alpha, v_\alpha) = \sum_{m=0}^{\infty} A_{2m+1}^{(2n+1)}(v_\alpha)\cos(2m+1)\alpha, \tag{A3}$$

$$\mathrm{se}_{2n+2}(\alpha, v_\alpha) = \sum_{m=0}^{\infty} A_{2m+2}^{(2n+2)}(v_\alpha)\sin(2m+2)\alpha. \tag{A4}$$

By substituting Eqs. (A1)–(A4) into Eq. (10), we obtain successive relations that determine the expansion coefficients. For $\{A_{2m}^{(2n)}\}$, as an example, we obtain the following relation:

$$\varepsilon A_0^{(2n)} - v A_2^{(2n)} = 0, \tag{A5}$$

$$(\varepsilon - 4)A_2^{(2n)} - v[2A_0^{(2n)} - A_4^{(2n)}] = 0, \tag{A6}$$

$$(\varepsilon - 4m^2)A_{2m}^{(2n)} - v[A_{2m-2}^{(2n)} - A_{2m+2}^{(2n)}] = 0 \ (m \geq 2). \tag{A7}$$

The orthogonality of the Mathieu functions is described by

$$\int_{-\pi}^{\pi} d\alpha\, \mathrm{ce}_l(v_\alpha, \alpha)\mathrm{ce}_{l'}(v_\alpha, \alpha) = \pi\delta_{ll'}, \tag{A8}$$

$$\int_{-\pi}^{\pi} d\alpha\, \mathrm{se}_l(v_\alpha, \alpha)\mathrm{se}_{l'}(v_\alpha, \alpha) = \pi\delta_{ll'}, \tag{A9}$$

$$\int_{-\pi}^{\pi} d\alpha\, \mathrm{ce}_l(v_\alpha, \alpha)\mathrm{se}_{l'}(v_\alpha, \alpha) = 0. \tag{A10}$$

## APPENDIX B: EXPLICIT FORM OF EQ. (14)

The explicit form of Eq. (14) can be obtained by expanding the state $\Psi(\xi, \eta, \tau^+)$ in terms of the Mathieu functions. Using these relations, the function (14) is expanded as

$$\Psi(\xi, \eta, \tau^+) = \sum_{l=0}^{\infty} \sum_{l'=0}^{\infty} D_{ll'} f_l(\xi, v_\xi) g_{l'}(\eta, v_\eta), \tag{B1}$$

where each type of the Mathieu function is abbreviated as

$$f_{2l}(\xi, v_\xi) = \mathrm{ce}_l(\xi, v_\xi), \tag{B2}$$

$$f_{2l+1}(\xi, v_\xi) = \mathrm{se}_l(\xi, v_\xi); \ l = 0, 1, 2\ldots. \tag{B3}$$

The definition of $g_{l'}(\eta, v_\eta)$ is the same as that of $f_l$. The expansion coefficients $\{D_{ll'}\}$ are calculated straightforwardly as

$$D_{ll'} = \int_{-\pi}^{\pi} d\xi \int_{-\pi}^{\pi} d\eta\, \Psi(\xi, \eta, \tau^+) f_l(\xi, v_\xi) g_{l'}(\eta, v_\eta). \tag{B4}$$

Substituting Eq. (B1) into Eq. (14), we obtain the explicit form of $\Psi(\xi, \eta, \tau^+ + t)$ as

$$\Psi(\xi, \eta, \tau^+ + t) = \sum_{l=0}^{\infty} \sum_{l'=0}^{\infty} \exp\left\{-\frac{i}{\hbar}[E_\xi^{(l)} + E_\eta^{(l')}]t\right\}$$
$$\times D_{ll'} f_l(\xi, v_\xi) g_{l'}(\eta, v_\eta). \tag{B5}$$

In actual calculations for Eq. (B5), the double summation with respect to $l$ and $l'$ can be truncated at a finite value, because the expansion coefficient $D_{ll'}$ rapidly decay with increasing $l$ and $l'$.

[1] H. Stapelfeldt and T. Seideman, Rev. Mod. Phys. **75**, 543 (2003), and references therein.

[2] J. Ortigoso, M. Rodríguez, M. Gupta, and B. Friedrich, J. Chem. Phys. **110**, 3870 (1999).

[3] J. J. Larsen, H. Sakai, C. P. Safvan, I. Wendt-Larsen, and H. Stapelfeldt, J. Chem. Phys. **111**, 7774 (1999).

[4] B. Friedrich and D. Herschbach, Phys. Rev. Lett. **74**, 4623 (1995); J. Phys. Chem. **99**, 15686 (1995).

[5] J. P. Heritage, T. K. Gustafson, and C. H. Lin, Phys. Rev. Lett. **34**, 1299 (1975).

[6] A. D. Bandrauk and L. Claveau, J. Phys. Chem. **93**, 107 (1989).

[7] P. M. Felker, J. Phys. Chem. **96**, 7844 (1992).

[8] T. Seideman, J. Chem. Phys. **103**, 7887 (1995); **106**, 2881 (1997); Phys. Rev. Lett. **83**, 4971 (1999).

[9] L. Cai, J. Marango, and B. Friedrich, Phys. Rev. Lett. **86**, 775 (2001).

[10] F. Rosca-Pruna and M. J.J. Vrakking, Phys. Rev. Lett. **87**, 153902 (2002).

[11] I. V. Litvinyuk, K. F. Lee, P. W. Dooley, D. M. Rayner, D. M. Villeneuve, and P. B. Corkum, Phys. Rev. Lett. **90**, 233003 (2003).

[12] I. Sh. Averbukh and R. Arvieu, Phys. Rev. Lett. **87**, 163601 (2001).

[13] M. Leibscher, I. Sh. Averbukh, and H. Rabitz, Phys. Rev. Lett. **90**, 213001 (2003).

[14] W. H. Oskay, D. A. Steck, and M. G. Raizen, Phys. Rev. Lett. **89**, 283001 (2002).

[15] R. A. Bartels, T. C. Weinacht, N. Wagner, M. Baertschy, C. H. Greene, M. M. Murnane, and H. C. Kapteyn, Phys. Rev. Lett. **88**, 013903 (2002).

[16] V. Kalosha, M. Spanner, J. Herrmann, and M. Ivanov Phys. Rev. Lett. **88**, 103901 (2002).

[17] R. Velotta, N. Hay, M. B. Mason, M. Castillejo, and J. P. Marangos, Phys. Rev. Lett. **87**, 183901 (2001).

[18] F. Haake, *Quantum Signature of Chaos* (Springer Verlag, 1991).

[19] H.-K. Park and S. W. Kim, Phys. Rev. A **67**, 060102 (2003).

[20] H. Shima and T. Nakayama, Phys. Rev. B **69**, 035202 (2004).

[21] Surface-mounted polar molecules having an in-plane dipolar moment and dipole rotors attached to a one-dimensional solid, respectively, are thought to be candidates for realizing arrangements (a) and (b) in Fig. 1.

[22] E. T. Whittaker and G. N. Watson, *A Course of Modern Analysis* (Cambridge University Press, Cambridge, 1962).

[23] M. Leibscher and I. Sh. Averbukh, Phys. Rev. A **65**, 053816 (2002).

[24] For arrangement (a), the initial state of the rotors just before the $\delta$ kick is set to $\theta_1(0) = \theta_2(0) = \pi/2$ or $-\pi/2$ with the same probability. For case (b), $\theta_1(0)$ can take any value with a uniform probability, while $\theta_2(0)$ is determined by the relation $\theta_2(0) = \pi - \theta_1(0)$. The initial angular velocity of $\theta_i$ immediately after the kick is determined by $\dot{\theta}_i(0^+) = -(P/I)\sin\theta_i(0)$ in both (a) and (b).

[25] H. Shima and T. Nakayama (unpublished).